Life Sciences 231 (2019) 116533

Contents lists available at ScienceDirect

Life Sciences

journal homepage: www.elsevier.com/locate/lifescie

Chronic intermittent hypobaric hypoxia attenuates skeletal muscle ischemia-reperfusion injury in mice

Wen-Jie Cheng[a,b,1], Xin Liu[c,1], Li Zhang[d], Xin-Qi Guo[e], Fu-Wei Wang[e], Yi Zhang[e], Yan-Ming Tian[e,f,*]

[a] Department of Anesthesiology, Tianjin Hospital, Tianjin 300000, China
[b] Graduate school, Hebei Medical University, Shijiazhuang, Hebei 050017, China
[c] Department of Neurology, Second Hospital of Xi'an Medical University, Xi'an, Shanxi 710038, China
[d] Department of Orthopedics, Third Hospital of Hebei Medical University, Shijiazhuang, Hebei 050051, China
[e] Department of Physiology, Hebei Medical University, Shijiazhuang, Hebei 050017, China
[f] Hebei Collaborative Innovation Center for Cardio-cerebrovascular Disease, Shijiazhuang, Hebei 050000, China

ARTICLE INFO

Keywords:
Chronic intermittent hypobaric hypoxia
Acute ischemia-reperfusion injury
Skeletal muscle
Inflammation
Apoptosis

ABSTRACT

Aim: The aim of this study was to investigate the protective effect of chronic intermittent hypobaric hypoxia (CIHH) against skeletal muscle ischemia-reperfusion (IR) injury and to determine the underlying mechanism.
Main methods: C57BL/6 mice were randomly divided into 3 groups: skeletal muscle IR injury group (IR), CIHH pretreatment following IR group (IR + CIHH), and sham operation group (Sham). The skeletal muscle IR injury model was induced by the unilateral application of a tourniquet on a hind limb for 3 h and then releasing it for 24 h. CIHH pretreatment simulating a 5000-m altitude was applied 6 h per day for 28 days. The functional and morphological performance of IR-injured gastrocnemius muscle was evaluated using contraction force, H&E staining, and transmission electron microscopy. IR injury-induced $CD68^+$ macrophage infiltration was assessed by immunofluorescence. TNFα levels in serum and muscle were measured by ELISA and western blotting, respectively. Apoptosis was examined by TUNEL staining and Cleaved Caspase-3 protein expression.
Key findings: Acute IR injury resulted in reduced contraction tension, morphological destruction, macrophage infiltration, increased TNFα levels, and apoptosis in gastrocnemius muscle. CIHH pretreatment significantly ameliorated contraction function and morphological performance in IR-injured skeletal muscle. In addition, CIHH pretreatment resulted in marked decreases in $CD68^+$ macrophage infiltration, TNFα levels, and apoptosis.
Significance: These data demonstrated that CIHH has a protective effect against acute IR injury in skeletal muscle via inhibition of inflammation and apoptosis.

1. Introduction

Skeletal muscle ischemia-reperfusion (IR) injury is a frequent clinical problem commonly seen in peripheral vascular injury, osteofascial compartment syndrome, and crush syndrome and leads to limb and remote multisystem organ dysfunction [1]. However, the mechanisms and course of skeletal muscle IR injuries are complex and involve multiple factors. It has been accepted that excessive inflammation response and apoptosis during IR causes cellular damage and dysfunction of skeletal muscle [2,3], and there is accumulating evidence that inhibition of the inflammation and apoptosis protects skeletal muscle from IR injury [4–6]. Although several agents, such as dexamethasone [7] and lipoxin [8], can effectively alleviate IR-injured skeletal muscle, new methods are still needed.

Chronic intermittent hypobaric hypoxia (CIHH) is a treatment for moderate hypoxia that simulates high-altitude conditions interrupted by normoxia. CIHH has been shown to have multiple beneficial effects on the body, such as protecting the heart against IR injury [9–12]. Our previous studies showed that CIHH (simulated atmospheric pressure equivalent to a 5000-m altitude for 28 days, 6 h daily) protected the heart against IR-induced damage. The mechanism involved CIHH decreasing the activity of beta-adrenoceptor in the right ventricular papillary muscle [13], enhancing cardiac anti-oxidation [14], strengthening the resistance against calcium overload [15], activating ATP-sensitive potassium channels, and inhibiting mitochondrial permeability transition pores [16], inhibiting endoplasmic reticulum stress

* Corresponding author at: Department of Physiology, Hebei Medical University, 361 East Zhongshan Road, Shijiazhuang, Hebei 050017, China.
E-mail address: tianyanming@hebmu.edu.cn (Y.-M. Tian).
[1] These authors contributed equally to this work.

https://doi.org/10.1016/j.lfs.2019.06.008
Received 28 March 2019; Received in revised form 25 May 2019; Accepted 3 June 2019
Available online 04 June 2019
0024-3205/

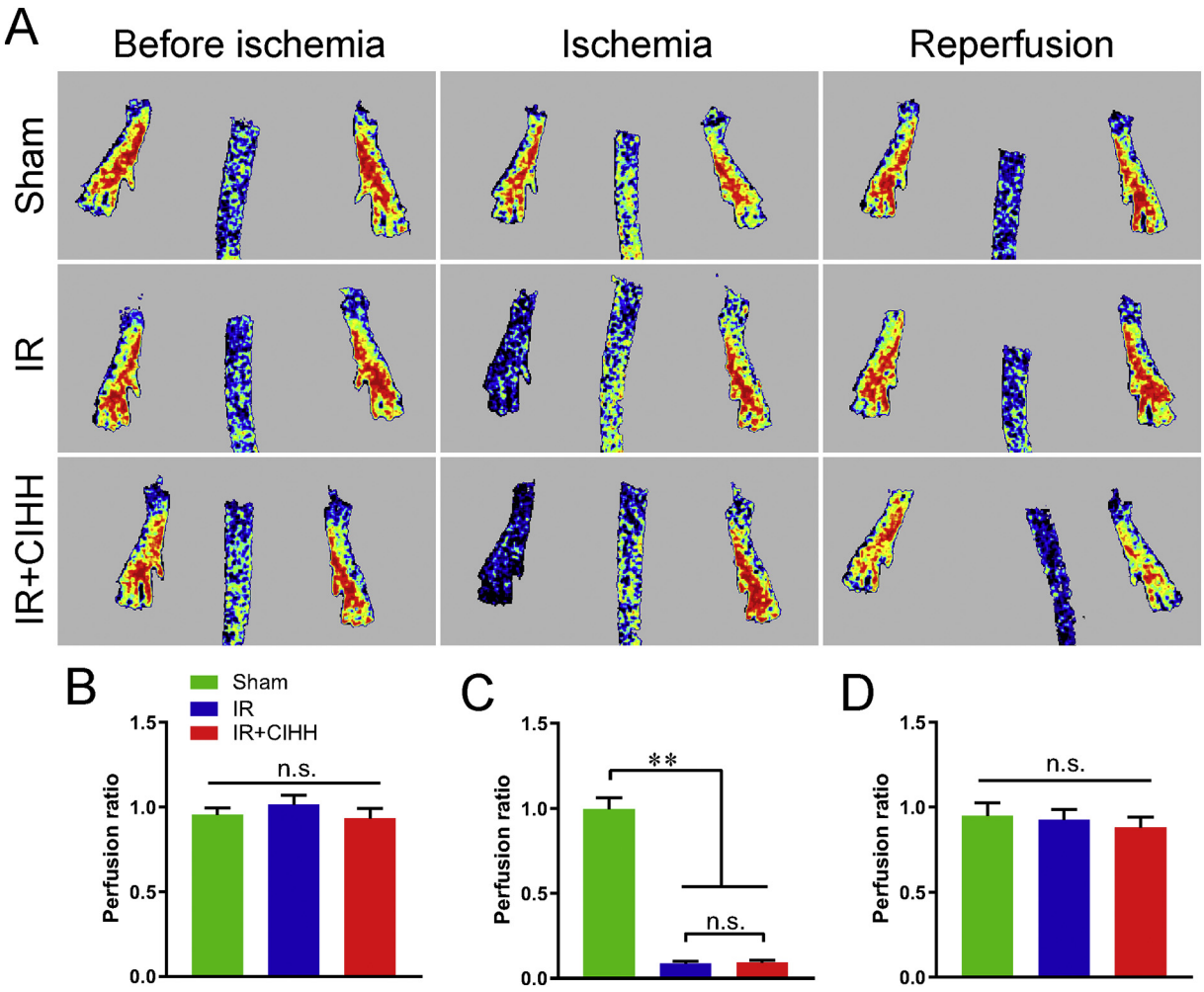

Fig. 1. Blood perfusion in the hind limbs following tourniquet-induced ischemia-reperfusion. Representative images of blood perfusion in mouse hind limbs obtained using laser speckle contrast imaging (A). Quantification of perfusion in the ischemic limb before ischemia (B), during ischemia (C), and during reperfusion for 24 h (D). Data are mean ± SEM, n = 6 in each group, and $^{**}P < 0.01$.

[17], and improving cardiac energy metabolism [18,19]. We recently found that in addition to cardiac protection, CIHH ameliorated skeletal muscle inflammation via inhibiting NFκB in rats with fructose-induced metabolic syndrome [20].

We therefore hypothesized that CIHH may protect skeletal muscle against IR injury. The aim of the present study was to determine whether CIHH would attenuate the structural and functional impairment of skeletal muscle after IR and preliminarily explore the mechanism involved.

2. Materials and methods

2.1. Animals

All experiments were performed on 10-week-old C57BL/6 male mice (body weight 20–30 g). Mice were housed in a room with controlled temperature (21 ± 1 °C) and humidity (50 ± 10%) and a fixed 12 h/12 h light/dark cycle and had free access to water and food. Animals were used in accordance with the Guide for the Care and Use of Laboratory Animals [43], and all techniques and procedures were reviewed and approved by the Hebei Medical University Institutional Animal Care and Use Committee.

2.2. Grouping and CIHH pretreatment protocols

A total of 60 mice were randomly divided into three groups according to random number table: skeletal muscle IR injury group (IR, n = 20), CIHH pretreatment and skeletal muscle IR injury group (IR + CIHH, n = 20), and sham operation group (Sham, n = 20). IR and IR + CIHH mice were subjected to 3 h of unilateral hind limb tourniquet ischemia followed by 24 h of reperfusion. IR + CIHH mice were exposed to hypobaric hypoxia simulating a 5000 m altitude (P_B = 404 mmHg, Po_2 = 84 mmHg) for 28 days, 6 h/day, in a hypobaric chamber, after which they were subjected to unilateral hind limb IR injury.

2.3. Acute hind limb IR injury model

The skeletal muscle IR injury model was constructed according to a modified version of a previously described method [7]. Briefly, the mice were anesthetized with isoflurane (4% induction followed by 1 to 1.5% maintenance) delivered in 100% O_2 by a nasal mask. Depth of anesthesia was determined by the absence of corneal and hindpaw withdrawal reflexes. The unilateral hind limb ischemia was induced by placing an orthodontic rubber band at the left hip joint using a McGivney hemorrhoidal ligator for 3 h followed by removal of the rubber band tourniquet for 24 h of reperfusion. Animals were maintained under anesthesia during the ischemia period, and the depth of

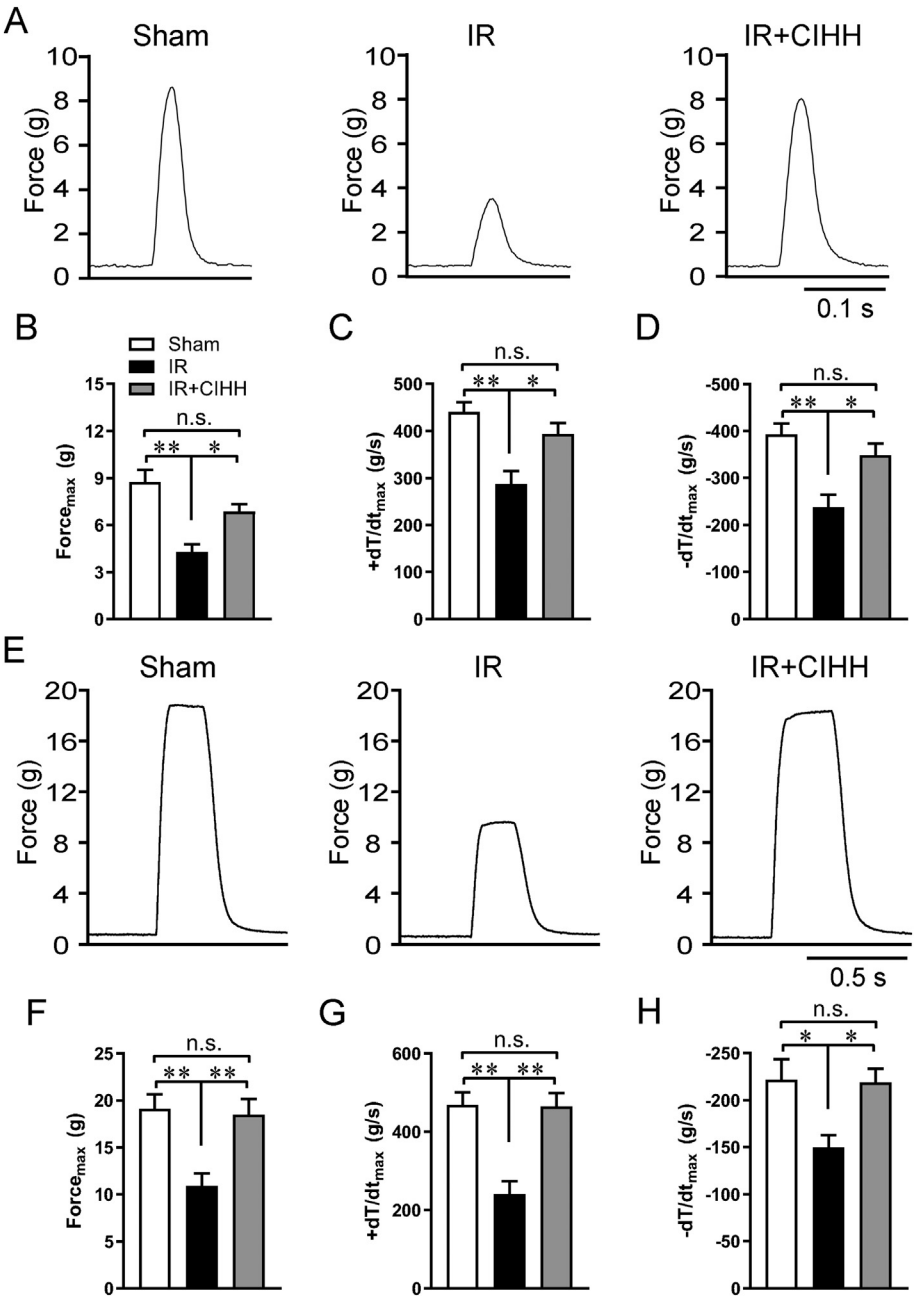

Fig. 2. CIHH strengthens contractile force in skeletal muscle after ischemia-reperfusion. Representative tracing of the single contraction assay induced via electrical field stimulation in an isolated gastrocnemius muscle (A). The maximum developed tension (B), the maximal rate of tension development (C), and the maximal rate of relaxation (D) in a single contraction. Representative tracing of the tetanic contraction in an isolated gastrocnemius muscle (E). The maximum developed tension (F), the maximal rate of tension development (G), and the maximal rate of relaxation (H) in tetanic contraction. Data are mean ± SEM, n = 6 in each group, $^{*}P < 0.05$, and $^{**}P < 0.01$.

anesthesia was monitored. A heating pad was used to maintain body temperature at 37 °C until the animals woke up. The tourniquet-induced IR injury was assessed by measuring blood flow to the hind limb.

2.4. Perfusion imaging

Limb perfusion was assessed using a real-time microcirculation imaging system. In general, mice were anesthetized with isoflurane and placed on a dark scanning surface. Perfusion of the dorsal surface of both the right and left hind limbs was measured using a blood perfusion imager (PeriCam PSI System, Sweden) based on laser speckle contrast analysis technology. Images were acquired before ischemia, during ischemia and 24 h after reperfusion. After acquisition, images of the mouse limbs were analyzed using PIMSoft (PeriCam PSI System). The value for the left ischemic limb was then normalized to that of the right (non-ischemic) limb to calculate the % of blood perfusion for each mouse.

2.5. Evaluation of muscle contractility

Mice were anesthetized by intraperitoneal injection of pentobarbital sodium (60 μg/g). Then, the left gastrocnemius muscle was rapidly excised and rinsed in cooled (4 °C) oxygenated Krebs-Henseleit solution. The muscle was mounted vertically in a 10 ml organ bath that was filled with Krebs-Henseleit solution containing (in mM) NaCl (118.0), KCl (4.7), $MgSO_4{\cdot}7H_2O$ (1.2), $CaCl_2$ (2.5), KH_2PO_4 (1.2), $NaHCO_3$ (25.0), and glucose (11.0), pH 7.4 ± 0.05, and maintained at 37 ± 0.5 °C and bubbled with 95% O_2/5% CO_2. A water bath was used to control the temperature of the bath solution. The proximal end of the gastrocnemius muscle was fixed, while the distal tendon was attached to a mechanical force transducer (AD Instruments, Australia). An initial tension of 1 g was applied to the muscle preparations, which were then left to equilibrate under these conditions for 60 min. The Krebs-Henseleit solution was changed every 15 min. A pair of platinum wire electrodes was placed longitudinally flanking the muscle, and the

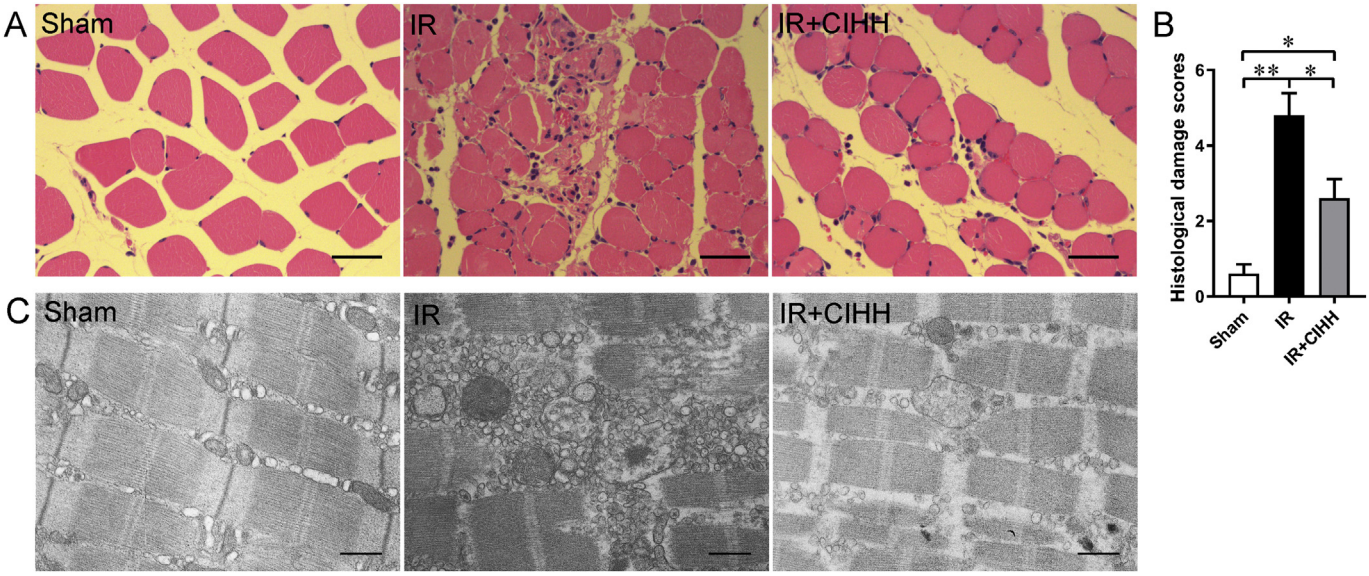

Fig. 3. Effect of CIHH on the morphology of skeletal muscle after ischemia-reperfusion. Representative photomicrographs of skeletal muscle tissue following H&E staining (A), scale bar = 30 μm. Quantification of histological damage scores determined by H&E staining (B). Ultrastructure of skeletal muscle analyzed by transmission electron microscopy (C), scale bar = 0.5 μm. Data are mean ± SEM, n = 5 in each group, $*P < 0.05$, and $**P < 0.01$.

contraction was induced via electrical field stimulation. The maximum force of single contraction was achieved by a square pulse with the following parameters: 5 V, 1 Hz, and 1 ms duration. The maximum force of tetanic contraction was achieved by a square pulse with following parameters: 5 V, 120 Hz, and 1 ms duration, for 30 cycles. The data were acquired and analyzed with LabChart 7 software (AD Instruments). The muscle contraction efficacy was assessed using maximum developed force ($Force_{max}$) and maximal rates of tension development and relaxation ($\pm dT/dt_{max}$).

2.6. Histological examination

The histological protocol has been described previously [21]. Briefly, the collected gastrocnemius muscle tissues were immerged in 4% paraformaldehyde for 48 h and then dehydrated in an ethanol step gradient. After they were embedded in wax, the tissues were sectioned at a 5 μm thickness using a microtome (Leica Microsystems, Germany), stained with hematoxylin-eosin (H&E), and imaged using a light microscope (Leica Microsystems). The degree of muscle damage was scored by a blinded pathologist according to previously published methods based on caliber variation, cytoplasmic fragmentation, and inflammatory cell infiltration. Each criterion was graded from 0 points for normal findings to 2 points for very distinctive findings [22].

2.7. Transmission electron microscopic examination

The gastrocnemius muscle samples were cut into cubes with a volume of 1 mm^3 and fixed in 4% glutaraldehyde for 1 h. After they were rinsed with 1 M phosphoric acid solution, the samples were fixed in 1% osmium tetroxide and dehydrated in a graded alcohol series. Then, the samples were embedded in epoxy resin and cut with an ultramicrotome (Leica Microsystems). After they were stained with uranyl acetate and lead citrate, the sections were viewed under a transmission electron microscope (S7500 Hitachi, Japan).

2.8. Determination of TNFα level in serum

Mice were anesthetized by intraperitoneal injection of pentobarbital sodium (60 μg/g). After the eyeball was removed, blood samples were collected from the eye socket. The collected blood samples were centrifuged at 3500 rpm for 10 min to obtain the serum. The tumor necrosis factor α (TNFα) concentration in serum was determined using a mouse ELISA kit (ABclonal Technology, USA).

2.9. Immunohistochemistry for CD68

The paraffin-embedded muscle blocks were cut into 5-μm-thick sections with a microtome (Leica Microsystems). They were mounted onto the gelatin-coated slides and allowed to dry overnight, and the sections were then deparaffinized, rehydrated, and subjected to antigen retrieval using a microwave. First, nonspecific antibody binding sites were blocked with 2% bovine serum albumin (BSA) and 0.3% Triton X-100 for 30 min at room temperature, followed by incubation with the primary antibody, rabbit polyclonal anti-CD68 (1:100; Servicebio, China), in 2% BSA overnight at 4 °C in a humidifying chamber. The sections were then incubated with the secondary antibody, goat anti-rabbit Cy3 (1:300, Servicebio), at room temperature for 1 h in the dark. Finally, after they were incubated with DAPI (Servicebio), the sections were mounted with Vectashield Antifade Mounting Medium (Vector Laboratories, USA) and photographed with a fluorescence microscope (DM6000B Leica Microsystems). The positive-stained cells were counted at 400× magnification in six random fields per section.

2.10. TUNEL assay

Apoptosis was detected using the terminal transferase-mediated deoxyuridine triphosphate-biotin nick end labeling (TUNEL) technique according to the manufacturer's instructions (Roche, USA). After they were deparaffinized and treated with 0.1% Triton X-100 for permeabilization for 20 min at room temperature, the paraffin sections were incubated with TUNEL reaction solution at 37 °C for 60 min. Then, the sections were rinsed with PBS three times for 5 min each and incubated with DAPI (Servicebio) at 37 °C for 10 min. After they were rinsed and covered, the sections were photographed using a laser scanning confocal microscope (FV1200 Olympus, Japan) and analyzed with Images-Pro Plus 6.0 software (Media Cybernetics Inc., USA). The apoptosis index, defined as the number of apoptotic cells/total number of cells counted, was used to determine the extent of skeletal muscle apoptosis. Six random fields at 400× magnification were selected per section.

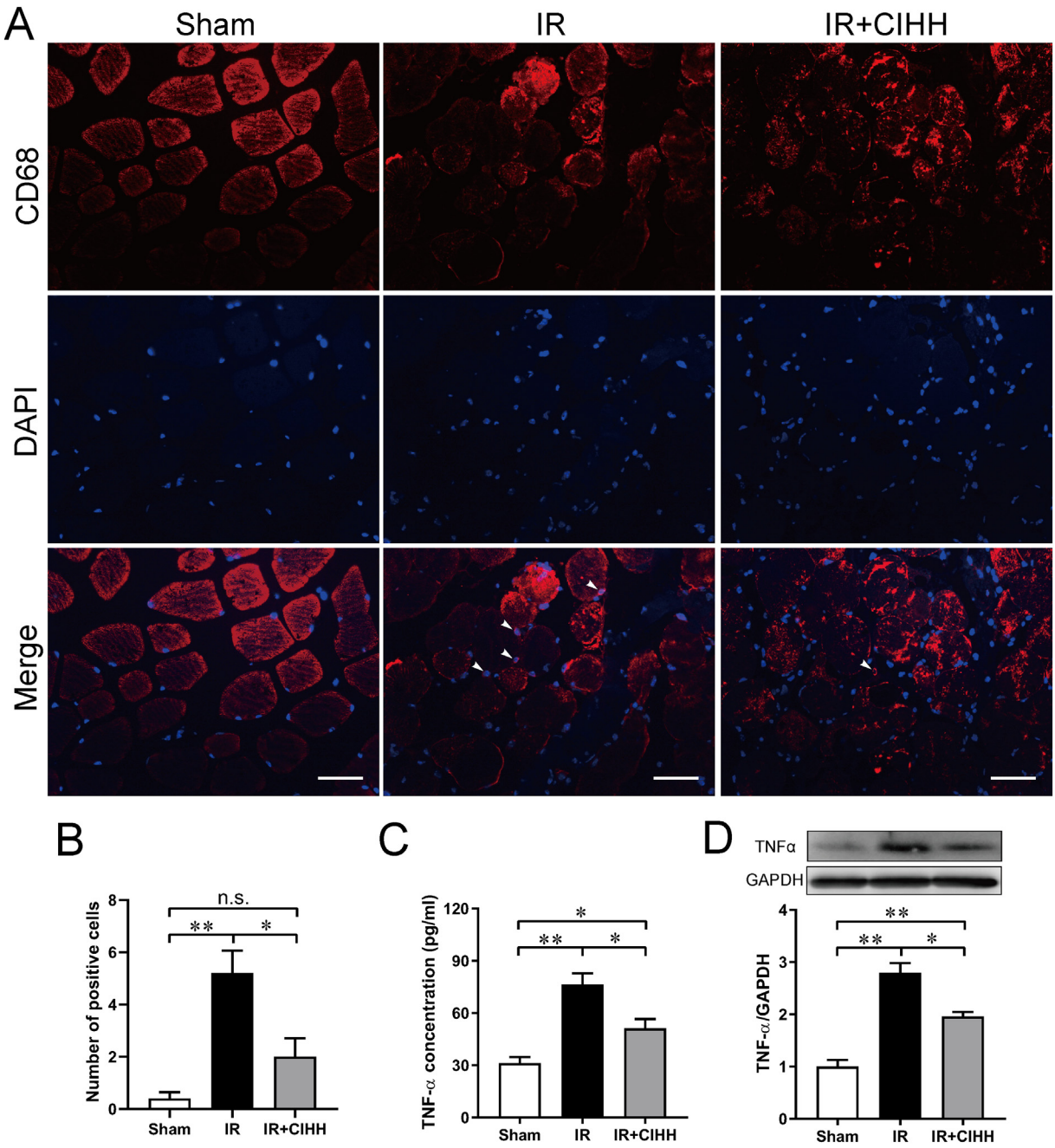

Fig. 4. CIHH mitigates inflammation in ischemia-reperfusion-injured muscle. The infiltration of CD68-positive macrophages (denoted by white arrows) was determined by immunofluorescence staining in injured muscle sections (A). CD68 was labeled red in the cytoplasm, and DAPI was labeled blue in the nucleus; scale bar = 30 μm. Quantification of CD68-positive cells in skeletal muscle at 24 h after IR (B). TNFα concentration in the systemic circulation (C) and protein expression in locally injured skeletal muscle (D). Data are mean ± SEM, n = 3–5 in each group, $*P < 0.05$, and $**P < 0.01$. (For interpretation of the references to colour in this figure legend, the reader is referred to the web version of this article.)

2.11. Western blotting analysis

Western blotting analysis was performed as described previously [23]. The muscle tissues were homogenized in a lysis buffer, and protein concentrations were determined by the bicinchoninic acid (BCA) protein assay (TIANGEN, China). Protein samples (50 μg) were separated by SDS-PAGE, transferred to a PVDF membrane (Millipore Corporation, USA), and blocked for 1 h with 5% (w/v) non-fat milk in Tris-buffered saline, followed by incubation with the primary antibodies anti-Cleaved Caspase-3 (1:500, Abcam, USA), anti-TNFα (1:1000, Abcam), anti-NFκB p65 (1:1000, Abcam), anti-TLR4 (1:500, Abcam), and anti-SIRT1 (1:1000, Abcam) overnight at 4 °C. The same membrane was stripped and re-blotted with anti-GAPDH (1:5000, HuaBio, China) for normalization. Blots were developed by the chemiluminescent method. The protein blots were quantified by densitometry using ImageJ software (NIH, USA), and the values were normalized to those of GAPDH.

2.12. Data analyses

Statistical analysis was performed with Prism version 7 (GraphPad Software Inc., USA). Values are presented as mean ± SEM. Data were assessed using one-way ANOVA followed by Tukey's tests for multiple comparisons. A value of $P < 0.05$ was considered statistically

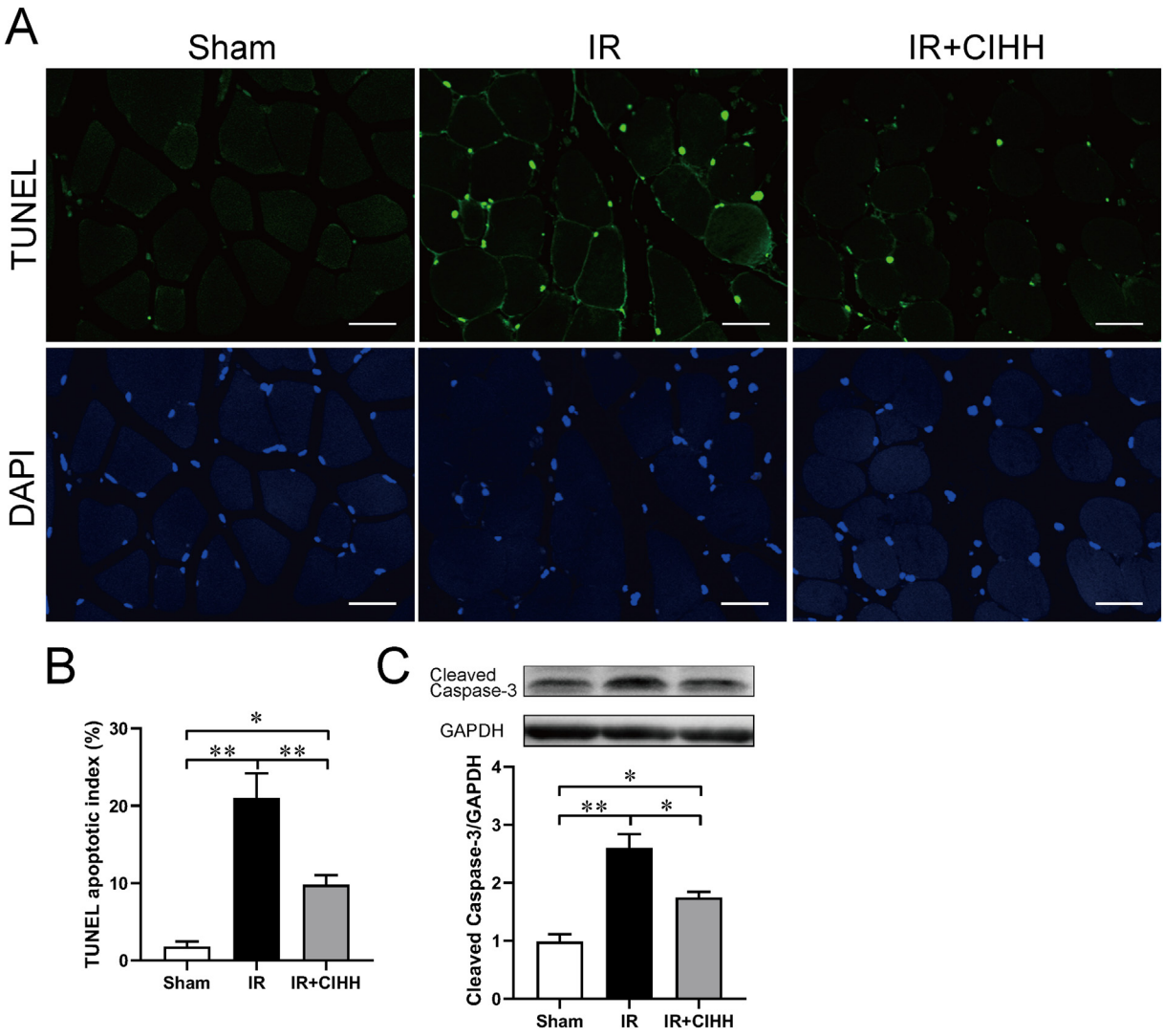

Fig. 5. CIHH extenuates apoptosis in ischemia-reperfusion-injured muscle. Representative images of apoptotic DNA breaks determined by TUNEL staining (A). TUNEL-positive nuclei were stained by immunofluorescent (green), and DAPI (blue) staining was used to label the nuclei; scale bar = 30 μm. The apoptotic index was analyzed using the numbers of TUNEL-positive nuclei relative to the total number of nuclei (B). The apoptosis marker Cleaved Caspase-3 was assessed by western blotting (C). Data are mean ± SEM, n = 3–5 in each group, $^{*}P < 0.05$, and $^{**}P < 0.01$. (For interpretation of the references to colour in this figure legend, the reader is referred to the web version of this article.)

significant.

3. Results

3.1. Evaluation of the tourniquet-induced IR model

The establishment of the tourniquet-induced hind limb ischemia-reperfusion injury model was verified by measuring hind limb blood flow before ischemia, during ischemia, and during reperfusion for 24 h. Blood flow images are presented in Fig. 1A. There was no difference in perfusion between the left and right hind limbs of the mice before ischemia in all three groups ($P > 0.05$, Fig. 1B). After placing the tourniquet, the blood flow in the IR and IR + CIHH groups dropped to about 8.8% and 9.1%, respectively (Fig. 1C), and no difference was found between the two groups ($P > 0.05$). After reperfusion for 24 h, the blood flow in the IR and IR + CIHH groups returned to baseline (Fig. 1D), and no difference was found between the two groups ($P > 0.05$). In the Sham group, there were no significant changes in blood flow before ischemia, during ischemia, and during reperfusion for 24 h (Fig. 1).

3.2. CIHH ameliorated muscle contraction in IR gastrocnemius muscles

Isolated gastrocnemius muscle contraction was triggered via electrical field stimulation. For a single contraction (Fig. 2A), the muscle contraction tension in the tourniquet-induced IR group was significantly lower than that in the Sham group (4.3 ± 0.5 g vs. 8.8 ± 0.8 g, $P < 0.01$, Fig. 2B). CIHH treatment improved muscle contraction tension in IR-injured gastrocnemius muscles ($P < 0.05$, Fig. 2B). Corresponding to the changes in contraction tension, the maximal rates of tension development and relaxation ($\pm dT/dt_{max}$) of gastrocnemius muscles in the IR group were lower than those in the Sham group ($P < 0.01$, Fig. 2C–D), and the $\pm dT/dt_{max}$ in the IR + CIHH group was significantly higher than that in the IR group ($P < 0.05$, Fig. 2C–D). The changes in tetanic contraction (Fig. 2E) were similar to those in the single contraction. The tetanic contraction tension and $\pm dT/dt_{max}$ in the IR group were significantly lower than those in the Sham group ($P < 0.05$–0.01, Fig. 2F–H), and CIHH significantly improved the tetanic contraction tension and $\pm dT/dt_{max}$ in IR-injured gastrocnemius muscle ($P < 0.05$–0.01, Fig. 2F–H). These results indicated that CIHH improved IR-induced muscle contraction dysfunction.

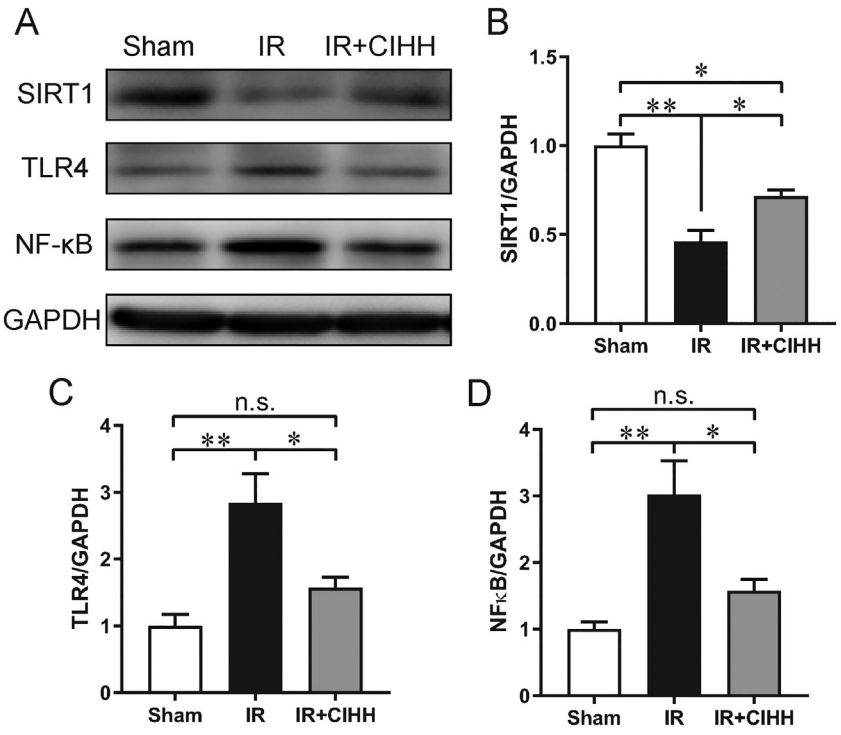

Fig. 6. Effect of CIHH on SIRT1, TLR4, and NFκB protein expression in ischemia-reperfusion muscle. Representative images of western blots (A) showing relative protein expression of SIRT1 (B), TLR4 (C), and NFκB p65(D) in gastrocnemius muscle. Data are mean ± SEM, n = 3 in each group, *$P < 0.05$, and **$P < 0.01$.

3.3. CIHH mitigated morphological injury in IR gastrocnemius muscles

The morphological injury of gastrocnemius muscles after IR was assessed by H&E staining and transmission electron microscopy. Optical microscopy evaluation revealed muscle cell swelling, sarcoplasm dissolution, and neutrophil infiltration in the IR group but not in the Sham group (Fig. 3A). CIHH significantly reduced muscle fiber injury after IR, with less sarcoplasm dissolution and neutrophil infiltration (Fig. 3A). Consequently, histological damage scores increased significantly in the IR group compared to those in the Sham group ($P < 0.01$, Fig. 3B), and CIHH decreased the histological damage scores in the muscular tissue following IR injury ($P < 0.05$, Fig. 3B). Electron microscopy evaluation revealed that myofibrils were arranged neatly in the Sham group, mitochondria and sarcoplasmic reticulum were clearly visible, and the mitochondrial membrane was relatively intact (Fig. 3C). In the IR group, myofibrils were disrupted and severely damaged, and mitochondria and the sarcoplasmic reticulum were swollen and dissolved (Fig. 3C). The ultrastructural performance assessed using electron microscopy in the IR + CIHH group was better than that in the IR group (Fig. 3C), which indicated that CIHH attenuated the morphological injury in IR gastrocnemius muscles.

3.4. CIHH relieved inflammation in IR gastrocnemius muscles

We measured macrophages and TNFα to evaluate the acute skeletal muscle IR-induced inflammation response. At 24 h after IR injury, a small number of macrophages migrated into the injured skeletal muscle, and these stained positively with an anti-CD68 antibody (Fig. 4A). The cell number of $CD68^+$ macrophages in the IR group was higher than that in the Sham group (5.2 ± 0.9 vs. 0.4 ± 0.2, $P < 0.01$, Fig. 4B). After CIHH pretreatment, the CD68-positive cells in the IR + CIHH group decreased compared to that in the IR group ($P < 0.05$, Fig. 4B). Likewise, the serum concentration and gastrocnemius muscle protein expression of TNFα significantly increased in IR-injured gastrocnemius muscle ($P < 0.01$, Fig. 4C & D). After CIHH pretreatment in the IR + CIHH group, IR-induced overexpression of TNFα in serum and gastrocnemius muscle markedly decreased ($P < 0.05$, Fig. 4C & D). The results indicated that CIHH attenuated the IR-induced inflammatory response.

3.5. CIHH attenuated excess apoptosis in IR skeletal muscles

TUNEL staining was used to evaluate the effect of CIHH on IR-induced apoptosis of skeletal muscle cells (Fig. 5A). As expected, IR injury markedly increased the apoptotic index in the IR group compared to that in the Sham group (21.0 ± 3.2% to 1.8 ± 0.7%, $P < 0.01$, Fig. 5B). After CIHH treatment, the rate of TUNEL-positive cells was significantly lower in the IR + CIHH group than in the IR group ($P < 0.01$, Fig. 5B). We also examined the apoptosis marker Cleaved Caspase-3. IR injury greatly increased the protein expression of Cleaved Caspase-3 ($P < 0.01$, Fig. 5C), and CIHH reversed this tendency ($P < 0.05$, Fig. 5C). These results suggested that CIHH can also decrease the level of apoptosis in skeletal muscle cells after IR injury.

3.6. Molecular mechanism by which CIHH attenuated skeletal muscle IR injury

To explore the molecular mechanism by which CIHH attenuated skeletal muscle IR-induced inflammation and apoptosis, the protein expression of silent information regulator 1 (SIRT1), Toll-like receptor 4 (TLR4), and NFκB p65 in IR-injured gastrocnemius muscle was detected by western blotting (Fig. 6A). The results revealed that after 3 h of ischemia and 24 h of reperfusion, SIRT1 protein expression significantly decreased in IR-injured muscle ($P < 0.01$, Fig. 6B), whereas in the CIHH pretreatment group, SIRT1 markedly increased ($P < 0.05$, Fig. 6B). Conversely, TLR4 and NFκB increased in IR-injured muscle compared to levels in the Sham group ($P < 0.01$, Fig. 6C & D). After CIHH pretreatment, the overexpression of TLR4 and NFκB markedly decreased ($P < 0.05$, Fig. 6C & D).

4. Discussion

In the present study, we prepared a mouse model of skeletal muscle IR injury using 3 h of ischemia and 24 h of reperfusion. In this model, IR caused functional and morphological damage to skeletal muscles. CIHH pretreatment significantly attenuated the IR-induced functional and morphologic damage, inflammatory response, and apoptosis in gastrocnemius muscles.

The hypoperfusion following IR injury has been described as the no-reflow phenomenon, which plays an important role in skeletal muscle IR injury. Many mechanisms are involved to the development of the no-reflow phenomenon such as interstitial edema formation and microvascular spasm [24]. Bonheur et al. found that the no-reflow appeared after 3 h but not 1 h of ischemia [25], which indicated that the severity of the no-reflow phenomenon depends on the duration of ischemia. Previous studies reported that after 3 h of ischemia, the perfusion recovered to about 30–40% of the baseline level [25,26] after 4 h of reperfusion and recovered to about 80–90% of the baseline level [27] after 24 h of reperfusion, indicating that after ischemia, the perfusion rate gradually recovered over time. In present study, after 3 h of ischemia and 24 h of reperfusion, the perfusion recovered to about 90% of the baseline level, which was consistent with the previous report [27]. Moreover, we also found that CIHH relieved the edema and inflammation but failed to improve the perfusion in IR-injured muscle. We speculate that this contradiction may be related to the observation time point and other factors, such as vasospasm and thrombus.

Although the mechanisms are complicated, accumulating lines of evidence suggest that inflammation plays a crucial role in the pathogenesis of skeletal muscle IR injury [4,28]. After IR injury, inflammatory cells infiltrate and promote the release of various inflammatory cytokines. The first inflammatory cells that arrive at the site of injury are neutrophils, which are eventually replaced by monocytes and then transformed into macrophages over 24–48 h [29]. In the present study, after 3 h of ischemia and 24 h of reperfusion, only a small number of $CD68^+$ macrophages migrated into the injured muscle, and the levels of TNFα, mainly produced by macrophages, increased in blood and local damaged skeletal muscle. After CIHH pretreatment, the number of $CD68^+$ macrophages and amount of TNFα markedly decreased. This indicated that IR induced severe systemic and local inflammatory responses, which were relieved by CIHH. Toll-like receptors (TLRs) are recognized as one of the main contributors to injury-induced inflammation. TLRs are activated by endogenous molecules released from damaged ischemic tissues, trigger downstream signaling cascades such as NFκB, and result in the release of various proinflammatory cytokines such as IL-1 and TNFα [30]. Moreover, a TLR4 mutant was found to reduce inflammation in hind limb IR injury [31]. To further explore the mechanism by which CIHH alleviated the inflammatory response in IR muscle, TLR4 and NFκB were examined. The results indicated that CIHH protected against IR-induced increases in TLR4 and NFκB levels, indicating the possible mechanism by which CIHH relieved IR-induced skeletal muscle inflammation.

Increasing lines of evidence show that exacerbated apoptosis participates in the damage of skeletal muscle IR [3,32]; however, the signaling pathways involved remain largely unknown. In the present study, apoptosis was evaluated by TUNEL staining, one of the most frequently used methods to evaluate apoptosis in tissue sections. We also examined a representative apoptosis marker, Cleaved Caspase-3, by western blotting, and the results were consistent with the TUNEL staining results. We found that IR muscle exhibited increased apoptosis and that CIHH significantly decreased the apoptosis. The SIRT1 signaling pathway has been shown to be associated with apoptosis during skeletal muscle IR injury [33]. To further explore the mechanism by which CIHH suppresses apoptosis in IR muscle, SIRT1 expression in skeletal muscle was analyzed. Our data showed a protective effect of CIHH against the apoptosis in skeletal muscle IR, partly through the activation of the SIRT1 signaling pathway.

To date, various beneficial effects of CIHH have been reported by different research groups [12,34,35]. For example, CIHH has been demonstrated to have preventive and therapeutic effects on several pathologic models, such as those for renal vascular hypertension [36], diabetes [23], cerebral ischemia [37], seizures [38], and aplastic anemia [39]. It was also reported that intermittent hypobaric hypoxia can be used to improve the aerobic capacity of athletes as a sport training method [40], treat patients with hypertension [41], and treat children with bronchial asthma [42]. Thus, we hypothesize that CIHH represents a non-pharmacological therapy to prevent or protect against lifestyle-related diseases in humans.

5. Conclusion

In summary, IR resulted in functional and morphological impairments in mouse skeletal muscles. Pretreatment with CIHH protected the skeletal muscle against acute IR injuries by inhibiting inflammation and apoptosis. Our results suggest that CIHH may represent a novel and efficacious treatment for IR-injured muscle tissue.

Author contributions

W-J C and XL performed the experiments. LZ and X-Q G analyzed the data. F-W W and YZ interpreted the results. Y-M T designed the experiment and drafted the article. All authors approved the version to be published.

Declaration of Competing Interest

No conflicts of interest, financial or otherwise, are declared by the authors.

References

[1] F.W. Blaisdell, The pathophysiology of skeletal muscle ischemia and the reperfusion syndrome: a review, Cardiovasc. Surg. 10 (2002) 620–630.
[2] R. Huda, D.R. Solanki, M. Mathru, Inflammatory and redox responses to ischaemia/reperfusion in human skeletal muscle, Clin. Sci. 107 (2004) 497–503.
[3] W.Z. Wang, X.H. Fang, L.L. Stephenson, K.T. Khiabani, W.A. Zamboni, Ischemia/reperfusion-induced necrosis and apoptosis in the cells isolated from rat skeletal muscle, J. Orthop. Res. 26 (2008) 351–356.
[4] D.W. Hammers, V. Rybalko, M. Merscham-Banda, P.L. Hsieh, L.J. Suggs, R.P. Farrar, Anti-inflammatory macrophages improve skeletal muscle recovery from ischemia-reperfusion, J. Appl. Physiol. 118 (2015) 1067–1074.
[5] G.C. Gaines, M.B. Welborn 3rd, L.L. Moldawer, T.S. Huber, T.R. Harward, J.M. Seeger, Attenuation of skeletal muscle ischemia/reperfusion injury by inhibition of tumor necrosis factor, J. Vasc. Surg. 29 (1999) 370–376.
[6] L.K. Mamedova, R. Wang, P. Besada, B.T. Liang, K.A. Jacobson, Attenuation of apoptosis in vitro and ischemia/reperfusion injury in vivo in mouse skeletal muscle by P2Y6 receptor activation, Pharmacol. Res. 58 (2008) 232–239.
[7] R.M. Corrick, H. Tu, D. Zhang, A.N. Barksdale, R.L. Muelleman, M.C. Wadman, et al., Dexamethasone protects against tourniquet-induced acute ischemia-reperfusion injury in mouse hindlimb, Front. Physiol. 9 (2018) 244.
[8] Zong H, Li X, Lin H, Hou C, Ma F. Lipoxin A4 pretreatment mitigates skeletal muscle ischemia-reperfusion injury in rats. Am. J. Transl. Res.. 2017;9:1139–[1]50.
[9] L. Wu, J.L. Tan, Z.H. Wang, Y.X. Chen, L. Gao, J.L. Liu, et al., ROS generated during early reperfusion contribute to intermittent hypobaric hypoxia-afforded cardioprotection against postischemia-induced Ca(2+) overload and contractile dysfunction via the JAK2/STAT3 pathway, J. Mol. Cell. Cardiol. 81 (2015) 150–161.
[10] H.C. Guo, F. Guo, L.N. Zhang, R. Zhang, Q. Chen, J.X. Li, et al., Enhancement of Na/K pump activity by chronic intermittent hypobaric hypoxia protected against reperfusion injury, Am. J. Phys. Heart Circ. Phys. 300 (2011) H2280–H2287.
[11] E.A. Herrera, J.G. Farias, A. Gonzalez-Candia, S.E. Short, C. Carrasco-Pozo, R.L. Castillo, Omega3 supplementation and intermittent hypobaric hypoxia induce cardioprotection enhancing antioxidant mechanisms in adult rats, Mar. Drugs 13 (2015) 838–860.
[12] J. Magalhaes, I. Falcao-Pires, I.O. Goncalves, J. Lumini-Oliveira, I. Marques-Aleixo, E. Dos Passos, et al., Synergistic impact of endurance training and intermittent hypobaric hypoxia on cardiac function and mitochondrial energetic and signaling, Int. J. Cardiol. 168 (2013) 5363–5371.
[13] Y. Guan, L. Gao, H.J. Ma, Q. Li, H. Zhang, F. Yuan, et al., Chronic intermittent hypobaric hypoxia decreases beta-adrenoceptor activity in right ventricular papillary muscle, Am. J. Phys. Heart Circ. Phys. 298 (2010) H1267–H1272.
[14] J.J. Zhou, Y. Wei, L. Zhang, J. Zhang, L.Y. Guo, C. Gao, et al., Chronic intermittent hypobaric hypoxia prevents cardiac dysfunction through enhancing antioxidation

in fructose-fed rats, Can. J. Physiol. Pharmacol. 91 (2013) 332–337.
[15] H.J. Ma, Q. Li, H.J. Ma, Y. Guan, M. Shi, J. Yang, et al., Chronic intermittent hypobaric hypoxia ameliorates ischemia/reperfusion-induced calcium overload in heart via Na/Ca2+ exchanger in developing rats, Cell. Physiol. Biochem. 34 (2014) 313–324.
[16] H.M. Bu, C.Y. Yang, M.L. Wang, H.J. Ma, H. Sun, Y.K. Zhang, (ATP) channels and MPTP are involved in the cardioprotection bestowed by chronic intermittent hypobaric hypoxia in the developing rat, J. Physiol. Sci. 65 (2015) 367–376.
[17] F. Yuan, L. Zhang, Y.Q. Li, X. Teng, S.Y. Tian, X.R. Wang, et al., Chronic intermittent hypobaric hypoxia improves cardiac function through inhibition of endoplasmic reticulum stress, Sci. Rep. 7 (2017) 7922.
[18] X. Li, Y. Liu, H. Ma, Y. Guan, Y. Cao, Y. Tian, et al., Enhancement of glucose metabolism via PGC-1alpha participates in the cardioprotection of chronic intermittent hypobaric hypoxia, Front. Physiol. 7 (2016) 219.
[19] S. Gu, H. Hua, X. Guo, Z. Jia, Y. Zhang, L.N. Maslov, et al., PGC-1alpha participates in the protective effect of chronic intermittent hypobaric hypoxia on cardiomyocytes, Cell. Physiol. Biochem. 50 (2018) 1891–1902.
[20] F. Yuan, Chronic intermittent hypobaric hypoxia ameliorated inflammation of skeletal muscle via inhibited NF-kappa B in rats with metabolic syndrome, Adapt. Med. 7 (2015) 83–89.
[21] Y.M. Tian, Y. Guan, N. Li, H.J. Ma, L. Zhang, S. Wang, et al., Chronic intermittent hypobaric hypoxia ameliorates diabetic nephropathy through enhancing HIF1 signaling in rats, Diabetes Res. Clin. Pract. 118 (2016) 90–97.
[22] O. Al-Sawaf, A. Fragoulis, C. Rosen, N. Keimes, E.A. Liehn, F. Holzle, et al., Nrf2 augments skeletal muscle regeneration after ischaemia-reperfusion injury, J. Pathol. 234 (2014) 538–547.
[23] Y.M. Tian, Y. Liu, S. Wang, Y. Dong, T. Su, H.J. Ma, et al., Anti-diabetes effect of chronic intermittent hypobaric hypoxia through improving liver insulin resistance in diabetic rats, Life Sci. 150 (2016) 1–7.
[24] S. Gillani, J. Cao, T. Suzuki, D.J. Hak, The effect of ischemia reperfusion injury on skeletal muscle, Injury 43 (2012) 670–675.
[25] J.A. Bonheur, H. Albadawi, G.M. Patton, M.T. Watkins, A noninvasive murine model of hind limb ischemia-reperfusion injury, J. Surg. Res. 116 (2004) 55–63.
[26] T.P. Tran, H. Tu, I.I. Pipinos, R.L. Muelleman, H. Albadawi, Y.L. Li, Tourniquet-induced acute ischemia-reperfusion injury in mouse skeletal muscles: involvement of superoxide, Eur. J. Pharmacol. 650 (2011) 328–334.
[27] H. Albadawi, R. Oklu, R.E. Raacke Malley, R.M. O'Keefe, T.P. Uong, N.R. Cormier, et al., Effect of DNase I treatment and neutrophil depletion on acute limb ischemia-reperfusion injury in mice, J. Vasc. Surg. 64 (2016) 484–493.
[28] M.L. Urso, Anti-inflammatory interventions and skeletal muscle injury: benefit or detriment? J. Appl. Physiol. 115 (2013) 920–928.
[29] B. Chazaud, M. Brigitte, H. Yacoub-Youssef, L. Arnold, R. Gherardi, C. Sonnet, et al., Dual and beneficial roles of macrophages during skeletal muscle regeneration, Exerc. Sport Sci. Rev. 37 (2009) 18–22.
[30] T.V. Arumugam, E. Okun, S.C. Tang, J. Thundyil, S.M. Taylor, T.M. Woodruff, Toll-like receptors in ischemia-reperfusion injury, Shock 32 (2009) 4–16.
[31] R. Oklu, H. Albadawi, J.E. Jones, H.J. Yoo, M.T. Watkins, Reduced hind limb ischemia-reperfusion injury in toll-like receptor-4 mutant mice is associated with decreased neutrophil extracellular traps, J. Vasc. Surg. 58 (2013) 1627–1636.
[32] J. Pottecher, C. Adamopoulos, A. Lejay, J. Bouitbir, A.L. Charles, A. Meyer, et al., Diabetes worsens skeletal muscle mitochondrial function, oxidative stress, and apoptosis after lower-limb ischemia-reperfusion: implication of the RISK and SAFE pathways? Front. Physiol. 9 (2018) 579.
[33] Y. Cheng, S. Di, C. Fan, L. Cai, C. Gao, P. Jiang, et al., SIRT1 activation by pterostilbene attenuates the skeletal muscle oxidative stress injury and mitochondrial dysfunction induced by ischemia reperfusion injury, Apoptosis 21 (2016) 905–916.
[34] L. Gao, L. Chen, Z.Z. Lu, H. Gao, L. Wu, Y.X. Chen, et al., Activation of alpha1B-adrenoceptors contributes to intermittent hypobaric hypoxia-improved post-ischemic myocardial performance via inhibiting MMP-2 activation, Am. J. Phys. Heart Circ. Phys. 306 (2014) H1569–H1581.
[35] C.C. Yang, L.C. Lin, M.S. Wu, C.T. Chien, M.K. Lai, Repetitive hypoxic preconditioning attenuates renal ischemia/reperfusion induced oxidative injury via upregulating HIF-1 alpha-dependent bcl-2 signaling, Transplantation 88 (2009) 1251–1260.
[36] N. Li, Y. Guan, Y.M. Tian, H.J. Ma, X. Zhang, Y. Zhang, et al., Chronic intermittent hypobaric hypoxia ameliorates renal vascular hypertension through up-regulating NOS in nucleus Tractus Solitarii, Neurosci. Bull. 35 (2019) 79–90.
[37] S. Zhang, Z. Guo, S. Yang, H. Ma, C. Fu, S. Wang, et al., Chronic intermittent hybobaric hypoxia protects against cerebral ischemia via modulation of mitoKATP, Neurosci. Lett. 635 (2016) 8–16.
[38] J.L. Zhen, W.P. Wang, J.J. Zhou, Z.Z. Qu, H.B. Fang, R.R. Zhao, et al., Chronic intermittent hypoxic preconditioning suppresses pilocarpine-induced seizures and associated hippocampal neurodegeneration, Brain Res. 1563 (2014) 122–130.
[39] J. Yang, L. Zhang, H. Wang, Z. Guo, Y. Liu, Y. Zhang, et al., Protective effects of chronic intermittent hypobaric hypoxia pretreatment against aplastic anemia through improving the adhesiveness and stress of mesenchymal stem cells in rats, Stem Cells Int. 2017 (2017) 5706193.
[40] G. Viscor, J.R. Torrella, L. Corral, A. Ricart, C. Javierre, T. Pages, et al., Physiological and biological responses to short-term intermittent hypobaric hypoxia exposure: from sports and mountain medicine to new biomedical applications, Front. Physiol. 9 (2018) 814.
[41] T.V. Serebrovskaya, E.B. Manukhina, M.L. Smith, H.F. Downey, R.T. Mallet, Intermittent hypoxia: cause of or therapy for systemic hypertension? Exp. Biol. Med. 233 (2008) 627–650.
[42] T.V. Serebrovskaya, R.J. Swanson, E.E. Kolesnikova, Intermittent hypoxia: mechanisms of action and some applications to bronchial asthma treatment, J. Physiol. Pharmacol. 54 (Suppl. 1) (2003) 35–41.
[43] PMID: 25121211, National Research Council, (1996), https://doi.org/10.1016/10.17226/5140.